Jan M. Zazula
CERN–SL/BT(TA), CH-1211 Geneva 23, Switzerland

Presented at the 2nd Workshop on Simulating Accelerator Radiation Environment, CERN, Geneva (October 9-11, 1995)

Abstract

Particle cascade simulations coupled with subsequent finite element thermal and mechanical calculations are an advanced, extremely useful, and sometimes the only available and reliable tool for solving practical as well as general engineering problems related to design and construction of accelerator components. The FLUKA Monte Carlo code and the ANSYS Finite Element system are extensively used by us for this purpose. In this paper we discuss physical assumptions made when using these programmes, modes of their applications, and their interface. Successful application of their mainframe for estimating spatial distributions and time evolution of temperatures and stresses in the accelerator domain are shown as examples: for the LHC and SPS beam dumps, and for the neutrino target at the SPS.

1 INTRODUCTION

In their conception, certain accelerator components must be specifically designed according to their thermal and mechanical reaction to continuous, pulsed or accidental absorption of high energy particle beams and their secondary showers. This may be achieved in so far, as detailed analyses may be performed of the subsequent particle cascade, heat transfer and structural deformation processes, induced by primary particles and (or) by their secondaries. In most cases the cross-coupled, time-dependent and nonlinear character of these processes must be considered. Depending on the nature of physical processes and on the type of equations to be solved, the stochastic or deterministic approach can be used. Two large advanced computer programs, the Monte Carlo (MC) code FLUKA [1] for the high energy processes, and the Finite Element (FE) ANSYS system [2]) for the thermo-mechanical analyses, have been extensively adopted, build into one mainframe, and applied by us.

Analysing of effects induced by high energy particles in matter involves almost all physical disciplines: from particle, nuclear and radiation transport physics [3] – through atomic, molecular and solid state physics [4] – to statistical physics and thermodynamics, mechanics of continuous media and elasticity theory [5]. A brief review of processes that transform energy of relativistic particles into temperatures and stresses is given in the next section of this report – with special emphasize given to their time scale. Because of their quantity and complexity, all those processes together cannot be treated with the highest possible level of detail, neither in theoretical considerations, nor in calculation precision, even by using systems of sophisticated computer programs like FLUKA and ANSYS; thus a choice of reasonable approximations plays a crucial role. In the last subsection of next section we review most important simplifications and limitations of the analyses that we have performed so far (see Refs. [6, 7, 8, 9, 10]). The strategy and technical realisation of these analyses are described in sections 3-5 of this paper. The examples and some their results are given in the last section. The first example illustrates how the energy scoring results, which are output of FLUKA programme, are transformed into time-dependent heat generation rates which are input for ANSYS system; the second example shows the transient heat transfer analysis with thermal radiation and convection effects; in the third example special attention is payed to the dynamic and quasi-static stress analysis. Each of these three examples is accompanied by a computer animation, shown in the oral session of this workshop. Most important parameters of the accelerator sub-systems, as they were taken for consideration in these examples, are summarized in Table 1 of this paper.

2 PHYSICS: FROM HIGH ENERGY BEAM TO PRESSURES, TEMPERATURES AND STRESSES

2.1 Primary propagation and cascade development

This first step is simulated with high level of detail (however, depending significantly on user options, and on an available computer time) by the FLUKA program used for all our analyses; the theoretical background can be found in the monograph [3]. Designing the accelerator components, we usually concentrate our interest in the region close to beam axis, where the spatial density of deposited energy reach highest values, and where it is dominated by electromagnetic showers and by ionization energy losses from fast charged particles. Thus the time scale is governed by the speed of primaries and relativistic secondaries that is comparable with the speed of light, so the cascade development and absorption processes exhibit in nanosecond time intervals after primary incidence, However, far from beam axis, or for special materials (*e.g.*, fissile), the energy deposition could be dominated by slow neutrons, and that would extend the considered time scale of energy deposition processes to times necessary for neutron thermalization, *i.e.*, microseconds.

Table 1: Most important parameters of the accelerator sub-systems, taken for consideration in the examples.

Beam parameters and system dimensions	LHC main dump		SPS	SPS/T9 target	
	dynamic analysis	thermal analysis	internal dump	slow extr.	fast extr.
Interception time[a]	0.25 ns	86 μs	6.4 μs	6 ms	10 μs
Intensity[b]	$1.7{\cdot}10^{11}$	$4.7{\cdot}10^{14}$	$2.4{\cdot}10^{13}$	$1.5{\cdot}10^{13}$	$1.3{\cdot}10^{13}$
Repetition time[c]	25.0 ns	3 h	16.8 s	14.4 s	7.2 s
Momentum	7 TeV/c		450 GeV/c	450 GeV/c	
Beam size[d] [mm^2]	2.3×2.3		9×1.7	1.2×1.2	
Material	C + Al		C + Cu	Be	
Lateral size [cm]	94		30	0.3	
Depth [cm]	800		430	110	
Reference reports	[8,10]		[6,7]	[9]	

[a] May be time interval of: single bunch (LHC dump), whole pulse (LHC and SPS dump), extraction duration (T9 target)
[b] Number of primaries (protons) per beam interception period (defined above)
[c] Time break between two subsequent beam interception periods (defined above)
[d] Widths at the horizontal and vertical half-maxima

2.2 Energy dissipation and equilibration processes in molecular and lattice scale

An amount of the cascade energy is counted as deposited if it cannot further propagate in form of shower components, *i.e.*, fast particles of energies above MC simulation energy cutoffs (and of ranges larger than bins of the energy-scoring mesh). At the second stage (after the primary passage and cascade development), and in region close to the beam axis, this energy occurs mostly in form of electrons and ions produced around charged particle tracks; far from the axis a significant fraction the stopped energy is carried also by heavy products and recoils of neutron-nuclear interactions. Because of their electrostatic field the ions attract adjacent molecules creating centers of local compression around [3] – partially releasing in mechanical form as an immediate pressure, and partially giving rise to energy of phonon vibrations of the solid lattice, thus increasing the temperature. This introduces some additional tenths of nanoseconds delay in transferring energy of the cascade into temperature and stress rise, and only after these highly in-equilibrium processes are finished, a macroscopic (molecular or solid) temperature can be defined as a reasonable characteristic of a certain volume of the matter. Fractions of the absorbed energy can be transferred as well to electric currents or to electromagnetic (thermal or microwave) radiation. This variety of atomic, molecular and solid state processes cannot unfortunately be analysed with any level of detail neither by FLUKA (even if one lowers energy cut-offs) nor by ANSYS. The partition of deposited energy between the thermal, mechanical and other degrees of freedom can be considered on a basis of the equation of state for solids [4]; however, the smaller are considered volumes and times, the more difficult it is to apply (see, *e.g.*, an interesting discussion in Ref. [11]). Ultimately, the only simple assumption made is that all the energy of cascade components falling below simulation thresholds is transferred totally, immediately and locally to further steps of the system evolution.

2.3 Propagation of mechanical energy (dynamic stresses)

Once pressure is created (either directly from molecular expulsion, or from secondary thermal expansion) its potential energy can remain for some time in a structure in the form of stresses, until it releases in form of mechanical work of structural deformations. The long-distance propagation of these deformations is then possible by elastic stress waves (see, *e.g.*, Ref. [11]). These phenomena, governed by the speed of sound propagation in solids, are still much faster than the heat transfer, and they exhibit in the microsecond time domain. Coupling between mechanical and thermal degrees of freedom can be realised on the base of thermo-elasticity theory [5], *i.e.*, assumption may be valid that any internal stresses occuring in the system have their origin only in thermal deformations of the structure and that they are proportional to strains (relative dilatations or frictions). This situation can be treated with satisfactory level of detail by mechanical and acoustic analysis modules contained in the ANSYS system. Providing that the spatial and time resolutions are fine enough, the dynamic strain and stress components (tensile or compressive) can be obtained. That is, however, not so easy to achieve with the FE method for large systems and for long time intervals, since a number of elements and of time steps is hardly limited by computer resources (CPU time and core to solve elemental equations, and an external memory to store and process elemental results, for many elements and sub-steps).

2.4 Thermal conduction, quasi-static stress

This step, if governed by thermal conduction, starts in a scale of milliseconds after energy absorption, and in case of heat convections by a cooling system or air, lasts even in a scale of many minutes. Any existing temperature gradients in the system are still accompanied by quasi-static stresses. We need to note, however, a special case of thermal radiation (*e.g.*, in internal cavities of an accelerator) for which the heat transfer or loss is instantaneous (speed of light). The analyses can be performed relatively easily by using the ANSYS system, but with some restrictions discussed in the next subsection. The thermal boundary conditions and mechanical constraints have essential influence on the results.

2.5 Restrictions and approximations

We do not pretend to discuss here the numerous approximations made in simulations of particle physics processes, and the precision or limitations of the high energy models, data (*e.g.*, high energy and nuclear cross-sections) and user options used in FLUKA. However, one needs to be aware that comparisons with measurements of absorbed dose distributions around accelerator beams have shown [12] that a mean accuracy (see the comment in Table 2) of not much better than 10% can be expected when estimating the spatial densities of energy deposited in large systems from Monte Carlo calculations with this code; this would be, however, a sufficient level for the analyses described in this paper.

From the point of view of any design study, the primary requirement is that accelerator components remain in the solid state, *i.e.*, below the temperature and pressure conditions critical for melting or even vaporization. If it is not possible to fulfill, first the choice of materials must be revised – or otherwise incorporation of a beam or cascade diluting system would be inevitable. If this condition is checked, further analyses are significantly simplified, since large density fluctuations would be significant for energy deposition results, and the cascade simulations would have to be repeated for each time step of the system evolution. We do not need to consider as well the hydrodynamic regime of energy transfer processes, phase transitions, chemical processes, *etc.*

In cascade simulations the cross sections can be assumed temperature-independent only until the thermal neutrons contribute negligible fractions of the total (maximal) *density* of the absorbed energy (note: neutrons, although abundant, especially in heavy materials, due to their penetration ranges are usually spread over large volumes). And the atomic properties significant for electromagnetic cascades are also assumed not to vary with temperature. In thermal and mechanical calculations for solids the temperature dependence of material properties must be always taken into account; therefore, nonlinear options are required in FE analyses. Last but not least, material properties of crystalic materials usually depend on direction; this need to be accounted for in preparation of the FE input data.

Very often a rough criterion of so called instantaneous temperature rise is used in design studies, *i.e.*, that all the energy deposited by the cascades is set equal to the enthalpy reserve of a material, and this is totally, immediately and locally converted into an adiabatic temperature rise. But of course the infinitely small time and space limits of the temperature do not exist, simply because of the microscopic structure of the matter (or, rather the concepts of nuclear or electronic temperatures would be more appropriate). Moreover, we learn from the basic thermodynamics that the temperature can be only defined for quasi-static processes and that is not the case for the first phase of physical phenomena following absorption of a high energy beam. Furthermore, we already know that at an early stage a significant fraction of energy is not used for local heating, but is released or stored in other forms (as pressure excursions, lattice defects, potential stress energy, *etc.*). As smaller is a volume (of a scoring bin or an element), the time after which an energy can be evacuated from it (*e.g.*, by a sound wave) becomes shorter, so shorter is the time (starting from a primary burst) for which this volume can be eventually considered as adiabatic. For a region smaller than beam size (a fraction of millimeter), and usual velocity of sound (few mm per μs) this time becomes a decimal fraction of microsecond, much less than an usual beam interception period (the time used for time integration of an initial heat). Ultimately, only the coupled thermo-mechanical analysis can overcome this problem. Note also that the specific heat at constant pressure, that is usually available from material property tables, must not be directly used for adiabatic estimates; the difference between the heat capacity at constant volume and at constant pressure is, anyway, not so large for many materials. In any case, an estimate of the maximum temperature in the system cannot be considered precise without specifying the volume size and the time interval that it concerns; the adiabatic result can be convenient for providing an upper (pessimistic) temperature limit.

For the mechanical calculations, it is important to verify that the elasticity limit of a material is not exceeded. Plastic deformation, and even phase transition and hydro-dynamic analyses are available in the ANSYS system; they are, however, extremely complicated and require special material data. Moreover, the mechanical constraints are usually an additional, external source of stresses. After an initial period of mechanical energy release, analyses of heat transfer and of the resulting thermal stresses can be separated and performed subsequently – reducing significantly the number of degrees of freedom taken simultaneously into account, and thus the number of equations solved for each time substep. For purely thermal analyses an initial heat accumulation can be time-integrated over a beam interception period – but only if this period is relatively long when compared to time of development and slowing down of a single cascade, and if it is short enough when compared to heat conduction time (see Table 1 for examples). Care must be taken also if the thermal contact surfaces between different materials can be assumed to be perfect.

3 MODEL GENERATION: FROM MC SCORING BINS TO FINITE ELEMENTS

3.1 Choice of the elements

First of all we note the principal difference between the MC scoring meshes and the FE meshes. For estimation of energy deposition from MC simulations the scoring bins play rather a passive role: they are simply the regular (cartesian, axi-symmetrical, *etc.*) volumes or phase-space regions that serve to accumulate a response of interest (*e.g.*, the deposited energy) from many individual cascade components, and to average it in order to express as a mean effect per one primary particle (and per unit phase-space volume). In the FE method the bins become the elements that play an active role: they deform with time, and they interact, each one with its neighbours, through the common points on their edges, called nodes.

Many kinds of elements are usually offered by sophisticated FE packages, and the choice of element type is an essential user task. The first element attribute to be decided on is a set of nodal degrees of freedom (DOF's); for our analyses the most suitable turn out to be the elements that have at least the following four coupled thermo-mechanical DOF's at each node: nodal temperature T, and the three components of the nodal translation (strain) vector (U_x,U_y,U_z). The next attribute is a suitable elemental input; the most convenient, for transferring results from MC energy deposition calculations, are the elements that allow for the internal energy input at each node, called also in FE terminology the internal heat generation rate (normalised as energy generated internally by any process, *e.g.*, by a particle cascade, per unit volume and per unit time). Coupling between thermal and mechanical DOF's means that this input is simultaneously and in proper fractions transformed (by a solution sub-step) to the temperature rise, as well as to the mechanical energy release. An output available from an element (*e.g.*, heat flow, stress components, *etc.*) must satisfy purposes of the analysis. The last but not least is the element dimensionality (*e.g.*, volume, surface, 2-dim. axi-symmetric, *etc.*), and capability to follow complicated boundary shapes (this generally depends on allowed number of nodes).

3.2 Mesh generation

One scoring mesh of FLUKA programme consists of bins of fixed size and shape. However, many overlapping meshes may be used, even in the same volume, some (coarse) for covering completely the system of interest, and some (fine) for concentrating scoring in relatively small regions of spatial maxima. In ANSYS system, only one mesh can cover a given volume or area, but the automatic meshing procedures allow for variable (user-specified or automatic) element size and shape; a mesh can be refined in regions of special interest by defining additional line divisions, concentration points, *etc.* This can significantly save on number of elements (number of equations to be solved), and thus memory and time for the calculations.

4 LOADS: FROM MC ENERGY DENSITY OUTPUT TO FE HEAT AND PRESSURE INPUT

The element and mesh consideration of the last section has led us to the following strategy in coupling of MC and FE calculations (shown also in schematic form in Figure 1):

1. To run the cascade simulation, using as many MC energy scoring bins and meshes as necessary to cover the system, and also, to provide good resolution at regions of spatial maxima. In particular, around a beam line the smallest transversal bin size for scoring the energy densities should be comparable with the size (Gaussian half-width) of the beam; larger bins cannot well reproduce maxima because of volume-averaging effect; however, smaller bins would often suffer from "statistical singularities": The energy cut-offs of the simulation must be consistent with bins, *i.e.*, they must be set up low enough to assure that the cascade components falling below these thresholds have ranges smaller than the spatial bin size. Until the central region of maximum energy densities is of particular interest, the simulation need not to be biased artificially.
2. To write a program (subroutine) that retrieves the energy density result at any arbitrary point of the system (defined by its coordinates), from the MC scoring output file. If necessary, this program unit must decide which MC scoring mesh is the most adequate at the actual region, end eventually interpolate the MC results between the actual position and center positions of the closest neighbouring bins.
3. To construct the solid geometry model for FE analysis, and to mesh it with concentration points/lines with respect to the beam and/or other critical regions of the system. After the mesh is completed, to write all node position on an external file.
4. To write the MC/FE interface program that performs the following tasks: (a) reads the node position file; (b) for each node position calls the subroutine retrieving an energy density results from MC output file (described in point 2); (c) finally, commands are written on an external file, in the ANSYS input format, assigning the energy density values to subsequent nodes.
5. To read in this external file by ANSYS, thus defining the nodal loads (they must be further normalized; see discussion in next section). The initial and boundary conditions need yet to be specified, and then the solution procedures can commence.

This method of coupling MC and FE analyses is not the only one possible, but it has turned out to be simple and effi-

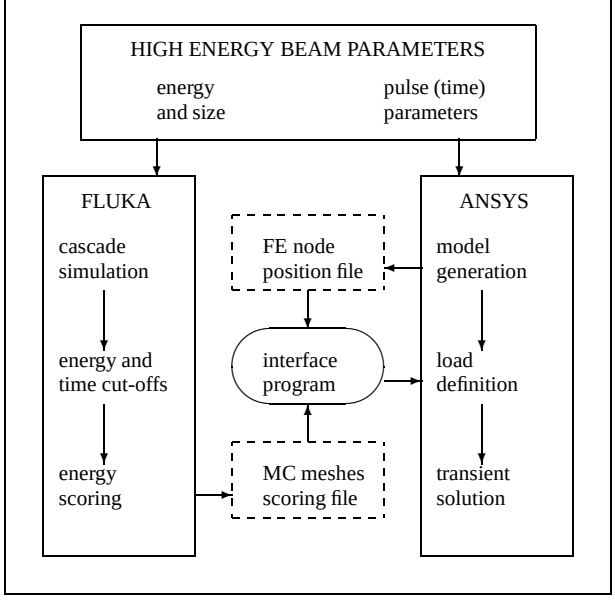

Figure 1: Strategy of coupling FLUKA and ANSYS systems for design of high energy accelerator components.

cient. No attempt was made to write a special program that could convert the Combinatorial Geometry geometry model of FLUKA into the solid model of ANSYS, or *vice versa*. However, this task is hard to be automise since both the FE and MC models may really need to be fairly approximated (*e.g.*, model dimensionality), and the reasonable approximations could be completely different at the levels of cascade simulations, and of temperature and stress calculations, so decisions must be left to the user's physical intuition and experience.

5 SOLUTION: FROM HIGH ENERGY BEAM PULSES TO TIME EVOLUTION OF THE SYSTEM

There are rather rare cases in the accelerator application domain where an analysed system attains thermal equilibrium such that steady-state solution procedures may be applied. In general, not only the spatial but also the time dependence of energy transfer (in both thermal and mechanical forms) must be taken into account. Firstly, different time-dependent states of a system are brought with the nature of different physical processes, with respect to their time scale (see the first section of this paper). Secondly, these primary time dependences overlap with the time dependence of the energy source itself, *i.e.*, of the high energy beam. This can be considered, to the last detail, as single particles coming instantaneously, but is most likely to be treated as many-particle spills of finite duration, like bunches (order of nanoseconds), buckets or extraction pulses (time duration can vary from nanoseconds to milliseconds). Note also that beam intensity, size and and even position (*e.g.*, in case of a sweeping system) can vary significantly with time.

Usual MC results are given as spatial densities of energy deposited per one primary; but they can only be estimated as an energy integrated over a certain time interval – usually counted from a moment when a primary hits the target, and usually with infinite upper time cutoff, just to include all contributions possible at any time (but energy cut-offs still remain). From the technical point of view, the time dependent FE analysis must be always divided into time steps, *i.e.*, periods small enough that the loads (and boundary conditions) that act on the system can be considered as constant, when expressed per unit time (eventually, they can be linearly ramped). Therefore in transient analysis the elemental input is not the energy density, but the energy generation rate (the internal energy provided per unit volume and per unit time). Thus, for transforming the MC energy scoring data into FE loads, a power deposited in the beam-intercepting step must be normalized by dividing the total number of primaries received in the step by the step duration. Of course in some other steps a source (beam) might be turned off, so for these steps the heat generation rate may be zero everywhere; however, the energy continues to dissipate, and the system evolves over a cooling-down period.

The next essential user's task (after selection of the element type) is to divide analysis into time steps and sub-steps, dependent on the solved problem, and on the required time resolution. For example, to observe the dynamic stress behavior (elastic waves) the beam intensity (and the respective heat generation rate) must be provided and transformed into the thermal input as averaged over time steps not longer than fractions of microseconds. On the other hand, if only the total performance of a cooling system of a continuously operating accelerator component (*e.g.*, target) is of interest, the integral beam intensity can be averaged over large periods of many seconds, or even approximately taken as a constant per unit time that leads to the steady-state analysis. Fortunately, for all thermal and most mechanical analyses required in the accelerator domain, the time effects of many single particles, many cascades and many bunches accumulate in relatively longer times of beam interception, and thus they can be integrated and averaged over the time length of a rectangular or trapezoidal beam spill.

6 EXAMPLES: FROM DESIGN PARAMETERS TO COMPUTER ANIMATIONS

6.1 Time-dependent profiles of power deposited by the LHC bunch

The twin LHC main beam dumps [13] need to be designed to absorb each of the two opposite high energy proton beams of momenta 7 TeV/c and intensities up to $4.7{\cdot}10^{14}$ protons. The total beam energy of 528 MJ, concentrated in the "hot spot" region of transversal dimension as small as 2.3 mm (half-maximum beam width), must be intercepted in time of 86 μs (revolution time). No solid materials could sustain the temperature and pressure conditions created if all these protons superpose the density of their deposited power (and of

their secondaries) along the same axis – thus a sophisticated beam sweeping system is a crucial element of the design [1].

A favorable material for construction of the dump core is graphite, of density 1.9 g/cm^3. A 600 cm long and 10 cm diameter graphite block can stop only about 42% of the total energy of the beam. The remaining 58% of the total beam energy is spread out, with a time delay, over large shielding volumes outside this radial and depth range, where concentrations of absorbed energy per unit mass and per unit time are 2 or 3 orders of magnitude lower.

The beam arrives each 25 ns in about 2835 bunches, each bunch of the intensity of $1.7{\cdot}10^{11}$ protons in a 0.25 ns spill (thus much shorter than inter-bunch interval). The primaries and fast secondaries are able to traverse 600 cm depth of the core in not less then 20 ns (speed of light limit). We have performed FLUKA simulations with time-dependent energy scoring, to learn that 99% of the total energy amount absorbed by graphite is deposited (more precisely, converted to electrons, charged hadrons and recoils of energies below the 1 MeV energy cutoff) during the first period of only 24 ns after a bunch incidence, *i.e.*, within a period comparable with a time gap between two bunches. Even if bunches are distributed over a sweep curve (this needs to be included in a circle of at least 200 mm diameter, to dilute sufficiently the maximum energy density levels) the inter-bunch space (order of 0.2 mm) cannot be as large as the lateral dimension of energy deposition profile (5 cm or more). The sound propagates in graphite with a velocity of 2.4 mm/μs. So a region as small as beam size (2.3 mm) can be eventually assumed adiabatic only for a time less that 1 μs. The power deposited from many bunches, converted to internal pressures, can interfere, giving rise to dynamic vibrations of the structure. During the overall absorption period (86 μs) shock waves can traverse distances longer than a diameter of the sweep. However, stress propagation may be attenuated, if the core structure is segmented, in both longitudinal and lateral directions.

The longitudinal profiles of power generated by one LHC bunch are shown in Figure 2 for a few different time intervals; they can be roughly described as a wave traversing longitudinally the core material, with the velocity of primary protons, and with some spatial and time dilution due to the secondaries. The energy densities per proton were scored in 15 scoring meshes, each one of identical R-Z bins (USRBIN option of FLUKA), but each of them with different upper time cutoffs (TCQUENCH option of FLUKA), increased successively by 2 ns, from 2 to 30 ns. To estimate power density at any spatial bin and for any time interval (*e.g.*, between 14 and 16 ns), the energy densities obtained with two subsequent time thresholds have to be subtracted (*i.e.*, the 14 ns results from the 16 ns results), and the differences have to be normalized per unit time (*i.e.*, by dividing by 2 ns); finally, this result is multiplied by the number of protons per bunch. Very illustrative is the computer animation, shown during the oral presentation on this workshop.

[1] Our calculations of the required magnetic field that could eventually dilute the cascade instead of the beam had shown [8] that no realistic magnet type can be constructed and installed in the dump area

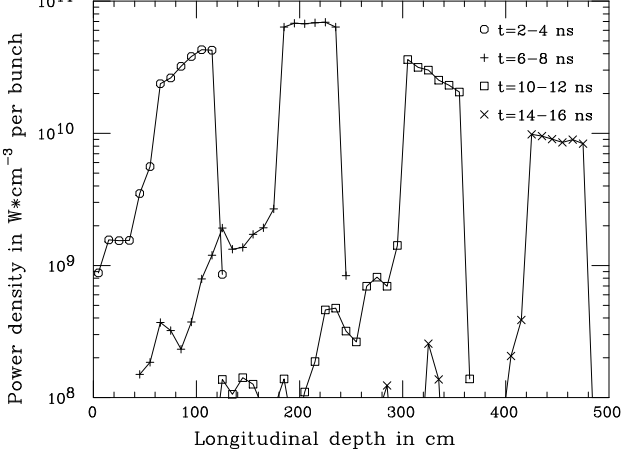

Figure 2: Longitudinal distributions of power deposited by the LHC bunch on axis of the graphite core of the beam dump, at four different time intervals.

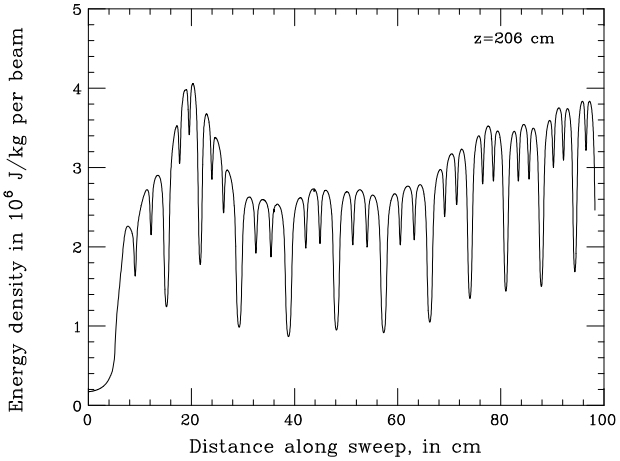

Figure 3: Density of energy deposited by the LHC beam in the graphite dump core, as a result of bunch distribution along a sweep contour.

The FE solid model of the core was meshed with regular elements with uniform longitudinal and azimuthal angle divisions, and with radial intervals increasing logarithmically from beam axis. The FLUKA results have been linearly interpolated at node positions (read in from an external file), and in time; the resulting nodal heat generation rate was read as input by ANSYS, and displayed in form of three-dimensional colour contours (no solution procedure is applied yet). One can see that even at an early stage of the analysis, the ANSYS graphical system, together with our interface program, can be readily used as an efficient and convenient tool for visualization and explanation of the MC simulation results.

The accumulated thermal part of the deposited energy simply adds in short time intervals (at any point and time, it superposes from all bunch positions, and from all earlier times) since the time necessary for heat release (few milliseconds) is still much longer then overall beam absorption time (< 0.1 ms). This is illustrated by Figure 3 that shows

spatial variations of the total energy density deposited by the LHC beam along a sweep contour, at the depth of longitudinal maximum (206 cm); the shape of the plot is a result of the bunch distribution pattern. The maximum tolerable temperature that occur in graphite just after the heating period, averaged over volumes not larger than 1 mm^3 (Gaussian σ-size of the beam), must not exceed about 2500 ^{o}C – this can be considered as a first rough criterion (but not only one) for accepting the sweep configuration. Regions laterally far from beam heat up not by the direct (cascade) energy deposition, but mostly by thermal conduction from the central hot region, and this occurs with a significant delay (several hundred seconds). Anyway, for mechanical reasons (quasi-static stresses, *etc.*), the temperature in the outside aluminum trench (about 35 cm aside the original beam axis) should not rise above 150^{o}C , at any time; this can serve as a criterion for deciding on the lateral core size. Cooling down time for all mass of the dump can take even hours, so if the absorber need to be at disposal for next dumping in earlier times, an additional cooling system must be installed. The design studies of the LHC dump that aim to answer these questions are continuing, in particular the thermal FE calculations are well advanced; a more complete set of the results will be reported elsewhere [10].

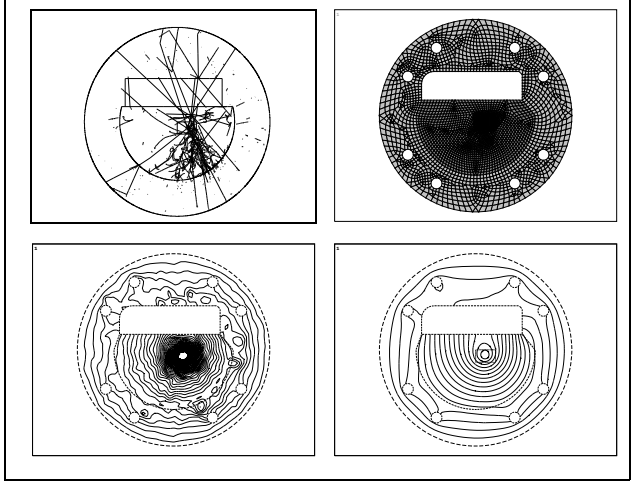

Figure 4: Analysis of a graphite plate of the SPS beam dump: (a) CG model for FLUKA simulations (upper left); (b) FE model for ANSYS analysis (upper right); (c) temperature contours after absorption of 6.4 μs beam pulse (bottom left); (d) steady-state isotherms (bottom right).

6.2 Temperature evolution in a graphite plate of the SPS beam dump

The internal beam dump (TIDV) of the SPS accelerator at CERN (see Table 1 for the beam parameters) needs some reconstruction in order to sustain the LHC injection regime. In our recent studies [6, 7] an optimized material choice and geometry layout was proposed. As a result of the particle cascade simulations (FLUKA) coupled with the transient heat transfer analysis (ANSYS), the spatial distributions of temperatures inside the modified dump were obtained together with their time evolution following absorption of the primary pulses. A beam sweeping system was roughly accounted for within the MC calculations, by sampling from a beam shape diluted over a rectangular area. The FE analyses of TIDV have been limited so far only to the thermal regime. Besides thermal conductivity, the selected elements account also for thermal radiation, as well as for thermal convection by cooling water.

Figure 4a-d of this paper show the same lateral cut of the TIDV (at the depth of the longitudinal maximum of deposited energy density, *i.e.*, about 95 cm in graphite) – including a central core plate, a passage for the circulating and injected beams, and the surrounding copper structure with cooling water channels (neglected for the cascade simulations) – as it appears at the four subsequent steps of the analysis: (a) the combinatorial geometry (CG) model assumed for the FLUKA run (a random sample of secondary particle tracks is also shown); (b) the FE model used in ANSYS (4205 thermal surface elements); (c) temperature contours (1^{o}C isotherms) at the time maximum (just after absorption of the 6.4 μs proton beam pulse); (d) the (hypothetic) equilibrium state isotherms, *i.e.*, obtained under assumption that the repetitive beam pulses must be absorbed continuously for a long time, with a constant heat generation input, obtained by averaging the beam intensity over the full beam cycle (16.8 s).

The time evolution of the temperature contours is animated for X-terminal display; observation of the isotherm development with time clearly shows, for example, radiation heating of the internal copper wall across the vacuum aperture. It turns out from the analysis that the maximum temperatures following beam absorption would not exceed 320^{o}C in graphite plates of the dump core, and 60^{o}C in the surrounding copper structure – assuming effective beam sweeping and external cooling conditions.

6.3 Stress development in a beryllium rod of the neutrino target

The heart of the SPS neutrino beam line, providing a source of pions, muons and subsequently produced neutrinos for the CHORUS and NOMAD experiments, is the T9 target consisting of 11 beryllium rods of 3 mm diameter and 10 mm length. In order to predict how many protons, assuming an available beam extraction regime, can be shot into the target without destroying it, the internal temperatures and stresses must be estimated with a certain precision, and this can be done only by theoretical calculations or simulations. This task was completed and the results are described in one of our recent notes [9].

The FLUKA simulation had shown that the first rod is the most critical, with respect to maxima and gradients (which lead to maximum stresses) of the absorbed energy density. This could be modeled with sufficient precision with 300 quadri-lateral axi-symmetric (2-dimensional) elements, of coupled therm-mechanical DOF's. The rod is cooled by gaseous helium, and free of mechanical constraints. The

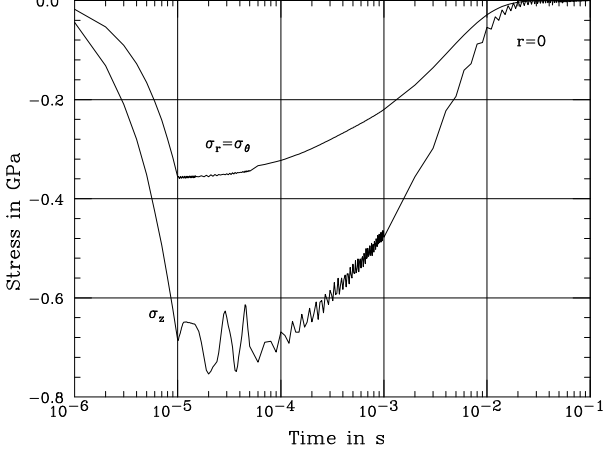

Figure 5: Time evolution of stress components (radial σ_r and longitudinal σ_z) at the point of maximum thermal load of the first Be rod of T9 target, submitted to fast extracted SPS beam (one cycle).

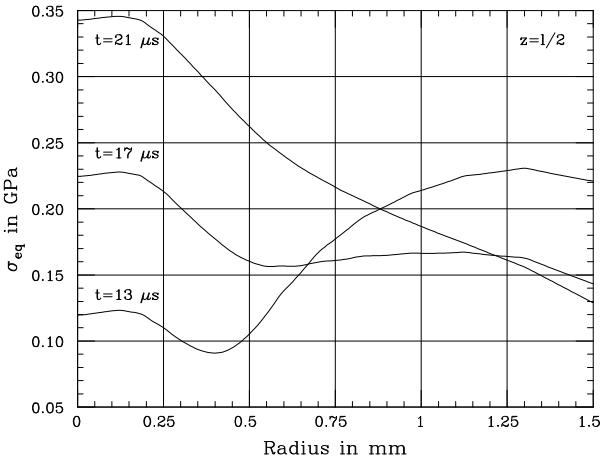

Figure 6: Equivalent stress along radius of the first Be rod of the T9 target, submitted to fast extracted SPS beam, shown at three different times of the first longitudinal shock wave.

analyses were made for the actual, slow extraction regime, and for an eventual future fast extraction regime (see Table 1). Although the obtained maximum temperatures for both cases are safely below the melting point, in case of the fast extraction the maximum equivalent stresses can slightly exceed the elastic limit of beryllium. The dynamic stress waves (both the longitudinal and radial components) generated in the case of the fast extraction had to be observed in time sub-steps as small as 0.1 μs (the radial vibration period was found to be 0.5 μs, and the longitudinal vibration period was 16 μs), but the dynamic stress amplitude was smaller than the quasi-static stresses (less than 25% in the longitudinal direction, and less than 1% in the radial direction).

The time evolution of the longitudinal and radial stress components for the fast extraction case, at the point of maximum thermal load (8.5 cm depth on the first rod axis), is reproduced from Ref. [8] in Figure 5 of this paper; note that the negative stress values mean that they are compressive. The wave behavior of the stresses is confirmed as well if they are plotted for different times as a function of longitudinal or radial position, see Figure 6 as an example. The time evolution of the deformed rod elements has been animated for X-terminal display, and provides a very spectacular illustration of the structure vibrations in two-dimensions.

Simplified one-dimensional analytical calculations for the Be rod of the SPS/T9 target were also completed [14], and they show close agreement with the FE method (see Table 2 of the quoted report). Successful operation over two years of slow extraction confirms reliability of the target.

7 CONCLUSIONS

Particle cascade simulations coupled with subsequent finite element thermal and mechanical calculations are an advanced, extremely useful, and sometimes the only one available and reliable tool for solving practical as well as general engineering problems related to design and construction of accelerator components. The FLUKA Monte Carlo code and the ANSYS Finite Element system are extensively used by us for this purpose. In this paper we discuss physical assumptions made when using these programmes, modes of their utilization, and their interface. In general application for the accelerator domain (except where simplifying assumptions may be valid), the time-dependent energy scoring is required in MC simulations, and the non-linear transient options with coupled thermo-mechanical degrees of freedom are required for FE analyses.

Successful application of their mainframe, for estimating spatial distributions and time evolution of temperatures and stresses in accelerator elements, is shown for three examples: of the main LHC beam dump (space and time distributions of power generated by cascades induced by a single bunch), of the internal SPS beam dump (two-dimensional heat transfer analysis with thermal radiation and cooling), and of the neutrino target at the SPS (dynamic and quasi-static stress analysis for axi-symmetric system). Basic criterion that decides on complexity of the analyses is the considered time interval of beam interception by a material. It can be well comparable with a time range characteristic for development and slowing down of a single cascade (nanoseconds) – as it is for the case of LHC bunch, with times of sound wave propagation (microseconds) – as it is for the case of fast SPS extraction, or with times of thermal conduction (miliseconds and more) – as it is for the case of slow SPS extraction.

One may ask what would be an ultimate precision of these calculation techniques. This must be of course closely dependent on the problem, on the required level of detail, on accuracy of the data, on the level of theoretical and numerical approximations and the following user's selection of analysis options. Moreover, use of these options is always limited by availability and quantity of input data (*e.g.*, cross-sections, material properties, *etc.*), as well as by computer resources (time, core, *etc.*). In Table 2 we summarize again different steps of the analyses, including their characteris-

Table 2: Rough estimation of a mean (overall) accuracy levels of obtained results (if estimated independently), together with their characteristic time domains, and most significant analysis parameters and material properties.

Type of result	Time range	Essential parameters	Material properties	Accuracy level	Comments
Spatial density of deposited energy or power	1-100 ns	Energy and time cut-offs scoring bins	Cross sections, el.-magn. cascade properties	$\sim 10\%$	Mean over detector positions; may be better on beam axis, but worse far off [12]
"Instantaneous" temperatures or pressures	< 1 μs	Beam interception period	Specific heat or enthalpy, density	$\sim 30\%$	Initial partition between thermal and other forms of energy is hard to determine
Dynamic stress frequencies and amplitudes	0.1-100 μs	Element type and size, sub-step times	Young moduli, Poisson's ratios, sound velocities	$\sim 20\%$	For small time intervals thermoelastic coupling may be not applicable
Quasi-static temperatures and stresses	> 0.1 ms	Boundary conditions, constraints	Conductivity and convection coefficients	$\sim 10\%$	Special care required for contact surfaces, thermal radiation, *etc*

tic time domains, most significant analysis parameters and material properties. For each step, we attempt to roughly estimate overall accuracy of the respective types of physical results, assuming that they are obtained independently (*i.e.*, without superposition of errors from previous steps). Experimental confirmation that this precision limits are not exceeded would be very encouraging, but direct measurement of temperatures and stresses in internal components of an operating accelerator are extremely difficult.

Acknowledgments

Many ideas, results and technical tools presented in this paper were elaborated together with my colleagues from CERN. I would like to mention especially: S. Péraire, M. Ross and E. Weisse from the SL/BT Group, and A. Fasso, M. Huhtinen and G.R. Stevenson from the TIS/RP Group.

8 REFERENCES

[1] A. Fassò, A. Ferrari, J. Ranft and P. R. Sala, "FLUKA: present status and future developments", Proc. of the *IV Int. Conf. on Calorimetry in High Energy Physics*, La Biodola (Is. d'Elba), Italy (Sept. 20–25 1993); Ed. A. Menzione and A. Scribano, World Scientific, p. 493 (1993).

[2] Swanson Analysis Systems, *Inc.*, "ANSYS (Revision 5.1)", SASI/DN-P511:51, Houston, USA (Sept. 30 1994).

[3] A.N. Kalinovskii, N.V. Mokhov and Yu.P. Nikitin, "Passage of high-energy particles through matter", Energoatomizdat, Moscow (1985); Am. Inst. of Phys. Transl. Series, New York (1989).

[4] G. Bush and H.Schade, "Lectures on solid state physics", Pergamon Press, Oxford (1974).

[5] L.D. Landau and E.M. Lifshitz, "Theory of elasticity", Pergamon Press, Oxford; 2^{nd} English Edition (1970).

[6] J.M. Zazula, M. Ross and S. Péraire, "A Preliminary Approach to Optimize the SPS Beam Dump for Sustaining the LHC Injection Regime", CERN SL/Note 94–52 (BT/TA), Geneva (July 1994).

[7] J.M. Zazula, M. Ross and S. Péraire, "Transient Temperature Distributions Effected by Dumping the SPS Beam (LHC Injection Regime)", CERN SL/Note 95–91 (BT/TA), Geneva (May 1995).

[8] J.M. Zazula, M. Gyr, G.R. Stevenson and E. Weisse, "A New Concept in the Design of the LHC Beam Dump", presented at the *PAC'95 Particle Accelerator Conf.*, Dallas, USA (May 1-5, 1995).

[9] J.M. Zazula, M. Ross and S. Péraire, "Thermo-Mechanical Effects Induced by SPS Beam in a Beryllium Rod of the T9 Neutrino Target", CERN SL/Note 95–90 (BT/TA), Geneva (August 1995).

[10] S. Péraire, M. Ross, G.R. Stevenson, E. Weisse and J.M. Zazula, "Design Studies of the LHC Beam Dump", CERN SL Report, to be published.

[11] Z. Tang and K. Anderson, "Shock Waves in P-bar Target", FERMILAB-TM-1763, Batavia, USA (Nov. 1991).

[12] A. Fassò, A. Ferrari, J. Ranft, P.R. Sala, G.R. Stevenson and J. M. Zazula, "Comparison of FLUKA simulations with measurements of fluence and dose in calorimeter structures", Nucl. Instr. and Meth. A 332 (1993) 459-468.

[13] The LHC Study Group, "Large Hadron Collider: The Accelerator Project", CERN AC/93–03 (LHC), Geneva (October 1993).

[14] S. Péraire, "Comportement Thermique et Mécanique d'une Cible en Beryllium Soumise à un Cycle d'Extractions Rapides", CERN SL/Note 95–54 (BT/TA), Geneva (May 1995).